A comparison of flow measurements around a series 60 (Cb=0.6), hull at yaw angles of 10 degrees and 35 degrees with CFD simulations
Molyneux, W. D.

National Research Council Canada   Conseil national de recherches Canada

Canada

DOCUMENTATION PAGE

REPORT NUMBER	NRC REPORT NUMBER	DATE
TR-2005-07		June 2005

REPORT SECURITY CLASSIFICATION	DISTRIBUTION
Unclassified	Unlimited

TITLE

A COMPARISON OF FLOW MEASUREMENTS AROUND A SERIES 60 (C_B=0.6), HULL AT YAW ANGLES OF 10 DEGREES AND 35 DEGREES WITH CFD SIMULATIONS

AUTHOR(S)

David Molyneux

CORPORATE AUTHOR(S)/PERFORMING AGENCY(S)

Institute for Ocean Technology, National Research Council, St. John's, NL

PUBLICATION

SPONSORING AGENCY(S)

Institute for Ocean Technology, National Research Council, St. John's, NL

IOT PROJECT NUMBER			NRC FILE NUMBER		

KEY WORDS		PAGES	FIGS.	TABLES
vertical axis propellers, escort tug		iv, 33	24	5

SUMMARY

The principal operational requirement for an escort tug is to be able to bring a loaded oil tanker to a controlled stop in the event of a steering or propulsion system failure on the tanker. The tug must be able to do this up to a maximum tanker speed of approximately 10 knots. The force required to control the tanker is generated by the tug using a combination of yaw angle (typically between 35 and 55 degrees) and azimuthing thruster angle (relative to the centreline of the tug). Using this approach it is possible to generate a force with a magnitude of up to two and a half times the bollard pull of the tug. The resulting force and its angle of application depend on the speed of the tanker, the delivered power of the tug and the direction of the thrusters on the tug. A popular and reliable choice of propulsion system for escort tugs is twin vertical axis propellers (VSP), which give very flexible control over the level of thrust and its direction. These propellers are typically fitted inside a protective cage.

ADDRESS	National Research Council Institute for Ocean Technology Arctic Avenue, P. O. Box 12093 St. John's, NL A1B 3T5 Tel.: (709) 772-5185, Fax: (709) 772-2462

National Research Council
Canada

Conseil national de recherches
Canada

Institute for Ocean
Technology

Institut des technologies
océaniques

A COMPARISON OF FLOW MEASUREMENTS AROUND A SERIES 60 (C_B=0.6), HULL AT YAW ANGLES OF 10 DEGREES AND 35 DEGREES WITH CFD SIMULATIONS

TR-2005-07

David Molyneux

June 2005

TABLE OF CONTENTS

LIST OF TABLES

LIST OF FIGURES

A COMPARISON OF FLOW MEASUREMENTS AROUND A SERIES 60 (C_B=0.6), HULL AT YAW ANGLES OF 10 DEGREES AND 35 DEGREES WITH CFD SIMULATIONS

INTRODUCTION

The principal operational requirement for an escort tug is to be able to bring a loaded oil tanker to a controlled stop in the event of a steering or propulsion system failure on the tanker. The tug must be able to do this up to a maximum tanker speed of approximately 10 knots. The force required to control the tanker is generated by the tug using a combination of yaw angle (typically between 35 and 55 degrees) and azimuthing thruster angle (relative to the centreline of the tug). Using this approach it is possible to generate a force with a magnitude of up to two and a half times the bollard pull of the tug. The resulting force and its angle of application depend on the speed of the tanker, the delivered power of the tug and the direction of the thrusters on the tug. A popular and reliable choice of propulsion system for escort tugs is twin vertical axis propellers (VSP), which give very flexible control over the level of thrust and its direction. These propellers are typically fitted inside a protective cage.

The hydrodynamic performance of three recent escort tug designs has been compared based on model scale measurements of hydrodynamic forces and moments (Allan & Molyneux, 2004). The principal particulars of the tugs described in this reference are given in Table 1. A sketch of the VSP hull is given in Figure 1. The large fin is typical of many modern escort tug designs, and is an important feature in the determining the magnitude of force developed. In escort operations, the tug is moving with the fin forwards.

Tug	VSP	ASD	Tractor
Appendage Option	RAL-Voith skeg	Hull & box keel	Hull, deep skeg
L_{wl}, m	38.19	39.89	38.19
B_{wl}, m	14.20	13.46	14.20
T (maximum), m	6.86	4.96	8.49
Δ, tonnes	1276	1187	1276
$A_{L,}$ m^2	161.4	157.5	161.0

Table 1, Summary of escort tug dimensions
(from Allan & Molyneux, 2004)

Figure 1, Profile view of VSP escort tug (from Allan & Molyneux, 2004)

Escort tug design to date has been evolutionary from previous operating practice and has not been based on detailed knowledge of the hydrodynamics of the situation. Predicting the flow patterns and resulting forces with Computational Fluid Dynamics (CFD) and validating the predictions against experiment data will help designers understand the flow around an escort tug. A review of the literature indicated, that although there were no specific cases of flow measurements around an escort tug, there were cases of detailed flow measurements for other ship types. Using this published data to validate CFD predictions of flow patterns for ships with large yaw angles is an important step in establishing the limitations of using CFD to assist escort tug design.

The tugs described above had waterline lengths between 38m and 40m. A tanker speed of 10 knots is equivalent to a Froude number of approximately 0.26 for the tug. At 8 knots the Froude number is approximately 0.21.

Two sets of flow measurement data were found for ship models with a yaw angle for speeds close to this range of Froude number (Longo and Stern, 1996, Di Felice and Mauro, 1999). Both sets of data were for the Series 60 hull, with a block coefficient of 0.6 (ITTC, 1987). This hull form is shown in Figure 2. The hull has very fine waterlines in the bow and stern and a midship section with a relatively large bilge radius. A summary of the principal particulars is given in Table 2. Even though the Series 60 Cb=0.6 hull is very different from the typical escort tug described above, using CFD to predict the flow around the hull and comparing the predictions to the measured flow patterns should be a useful step in understanding the hydrodynamics of a hull with a yaw angle. In particular, the focus of the study should be on the flow around the mid-section of the ship, away from the influence of the fin and other effects caused by the bow and the stern.
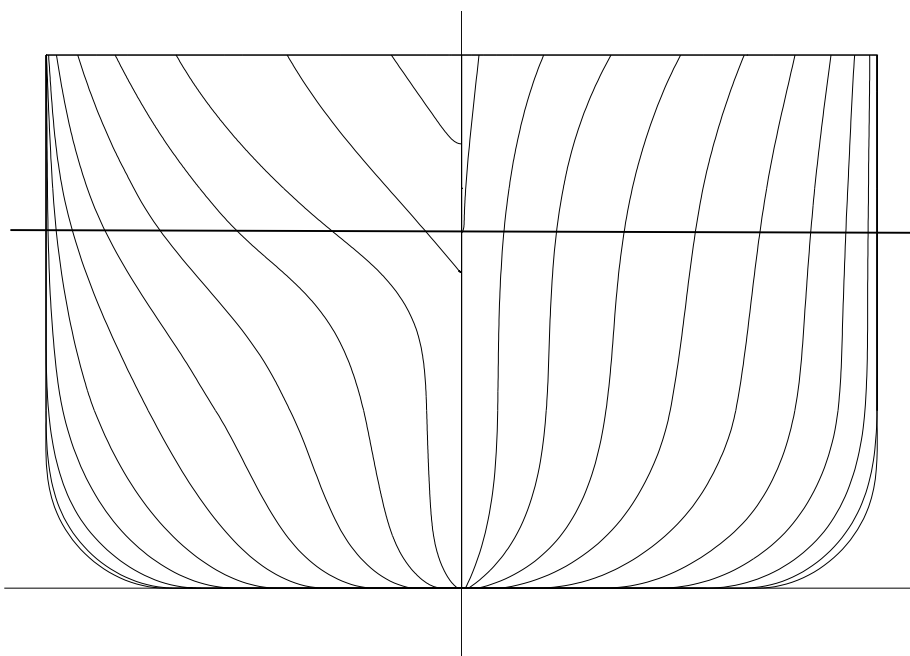
Figure 2, Series 60, C_B=0.6, Body plan for hull showing 21equally spaced sections along waterline length

	Full scale	Iowa model	INSEAN model
Length, BP, m	121.92	3.048	1.219
Beam, m	16.256	0.406	0.163
Draft, m	6.502	0.163	0.065
C_B	0.6	0.6	0.6
C_M	0.977	0.977	0.977
Scale		1:40	1:100

Table 2, Principal Dimensions for Series 60, C_B=0.6

EXPERIMENT DATA FOR FLOW AROUND SERIES 60 HULL WITH YAW

The data from the two sets of experiments are not directly comparable, because they were measured on two different axis systems. Each system was chosen for valid reasons based on the nature of the experiments and the facility in which the experiments were carried out. Longo and Stern chose a ship based axis system for measurements in a towing tank. In this system, all measurements were made relative to an axis based on ship coordinates. The three orthogonal axes were defined relative to the centreline of the ship. In this system, undisturbed flow will cross the measurement plane at an angle. Di Felice and Mauro chose a measurement axis system based on the flow direction, since they did their experiments in a cavitation tunnel, and the measurement system was fixed in the tunnel

3

coordinates, normal to the centreline of the tunnel. The measurement plane was normal to the undisturbed flow direction. In this system, undisturbed flow will be perpendicular to the measurement plane. The two axis systems are illustrated for the Series 60 hull at 50%L for 35 degrees of yaw in Figure 3.
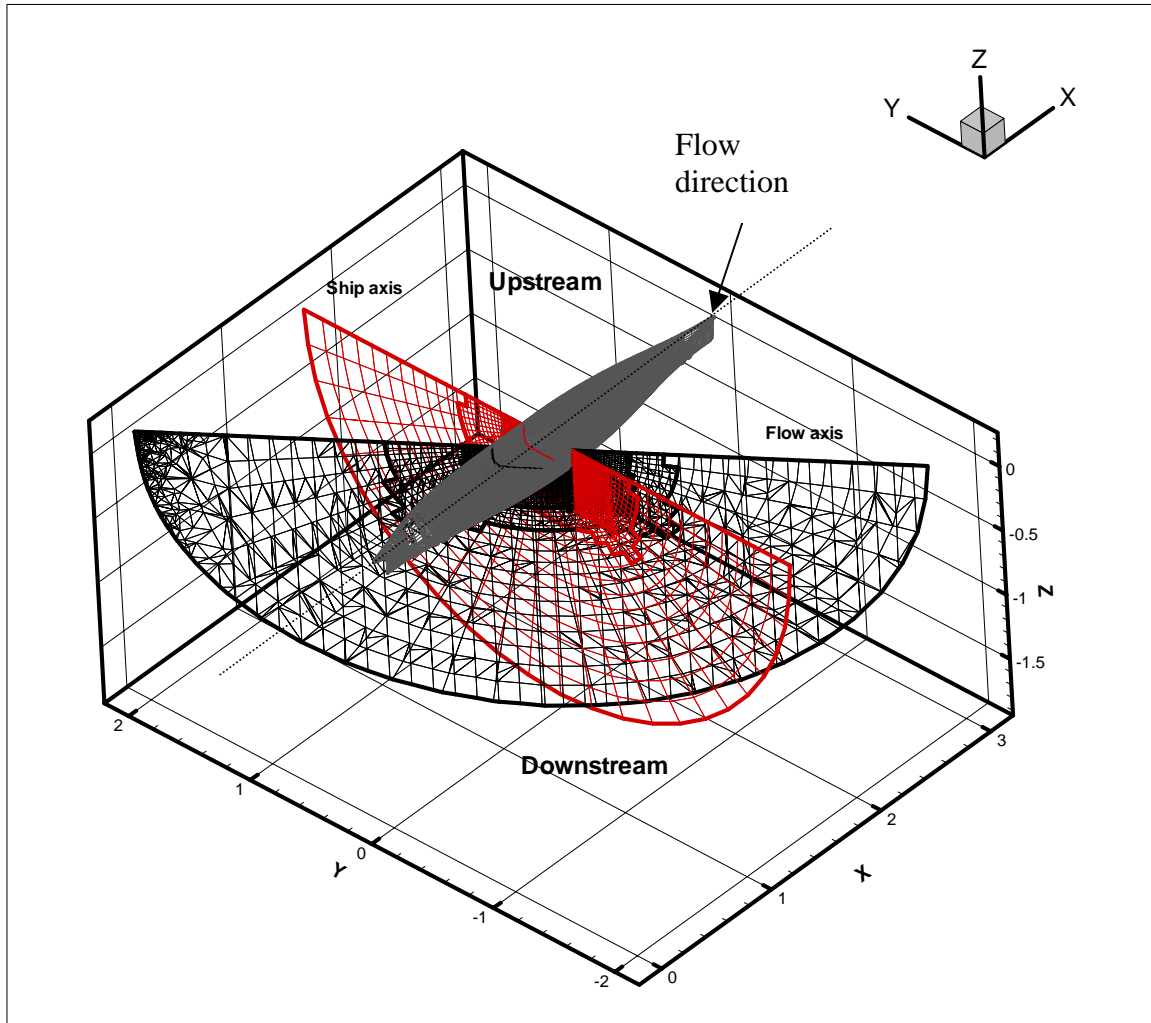
Figure 3, Measurement planes for Series 60, Cb=0.6 at 50%L,
Ship based coordinates in red, flow based coordinates in black

Pitot Tube Data for Yaw Angle of 10 Degrees

An extensive flow survey around a model of the Series 60, C_B=0.6 hull was made using five-hole pitot tubes for zero yaw angle (Toda et al., 1992, Longo et al., 1993) and with a 10 degree yaw angle (Longo and Stern, 1996). The experiments were carried out to determine the influence of waves created by a surface-piercing hull on its wake and boundary layer and to provide detailed measurements of the flow field for validating CFD methods. Mean velocity and pressure measurements were made for two Froude numbers (0.160 and 0.316) at multiple sections from the bow to the stern, and into the

4

near wake at the stern. The two speeds were chosen to give the effects of waves on the flow.

A Cartesian measurement grid was used with the origin at the intersection of the forward perpendicular and the static waterline. The x-axis was positive towards the stern, the y-axis was positive to starboard and the z-axis was positive upwards. Velocities in the x, y and z direction were referred to as u, v and w respectively. Results were non-dimensionalized using model length (between perpendiculars) L, carriage velocity U and fluid density ρ. Two models were tested, at scales of 1:40 and 1:66.7.

Data from the experiments was presented as total head and axial (u) velocity contours, cross plane (v, w) velocities and pressures and axial vorticity contours. The y-z planes were at locations of 0, 0.1, 0.2, 0.4, 0.6, 0.8, 0.9, 1.0, 1.1 and 1.2L for each of the two Froude numbers. Wave profiles at the hull surface, contours of wave elevation and wave slope were also measured. Pressure measurements with the pitot tubes were made at between 200 and 350 data points per section.

Wave profiles at the hull were measured at more locations than the pressures. Wave elevation was measured using an array of wave probes fixed in the tank axis system, referred to in the paper as global elevations. Wave elevation close to the model was measured from a moving wave probe on the towing carriage, and this was referred to as local elevation. For the zero yaw case, the results presented were based on the combination of approximately 4000 carriage runs.

The work at 1:40 scale was expanded to include steady yaw angles up to 10 degrees (Longo & Stern, 1996). Forces and moments were measured for yaw angles from zero to 10 degrees at intervals of 2.5 degrees. Wave profiles at the hull surface and wave elevations were measured at yaw angles of zero, 5 and 10 degrees. Detailed pressure measurements were made at 10 degrees only. The methods used were essentially similar to the ones discussed above, with some minor changes. The biggest difference was that the range of the local wave surface measurements had to be extended, since the projected beam of the ship was wider, due to the yaw angle. Also, measurements were required on both sides of the hull, since the flow was no longer symmetric about the centerline.

The more complex flow around the yawed hull required a more precise spatial definition than the symmetric flow, and so data density for measurements was increased to between 800 and 1500 points per y-z plane. The measurement grid for the case with 10 degrees yaw is given in Figure 4.

The results of the experiments for the zero yaw and the yawed case are available from the web site of the Computation Ship Hydrodynamics Laboratory at the University of Iowa (http://www.iihr.uiowa.edu/~towtank/series60bare.htm). For the purposes of this research, these data were re-plotted as contours of longitudinal flow velocity, u (non-dimensionalized by the free stream speed, U) and vectors of in-plane flow components (v-w, also non-dimensionalized by the free stream speed, U) for selected sections along

the hull. The sections chosen were 20%L, 40%L, 60%L and 80%L (measured aft from the forward end of the waterline). These locations were chosen to cover the mid-body section of the hull. Results are shown plotted in Figures 5 to 8.
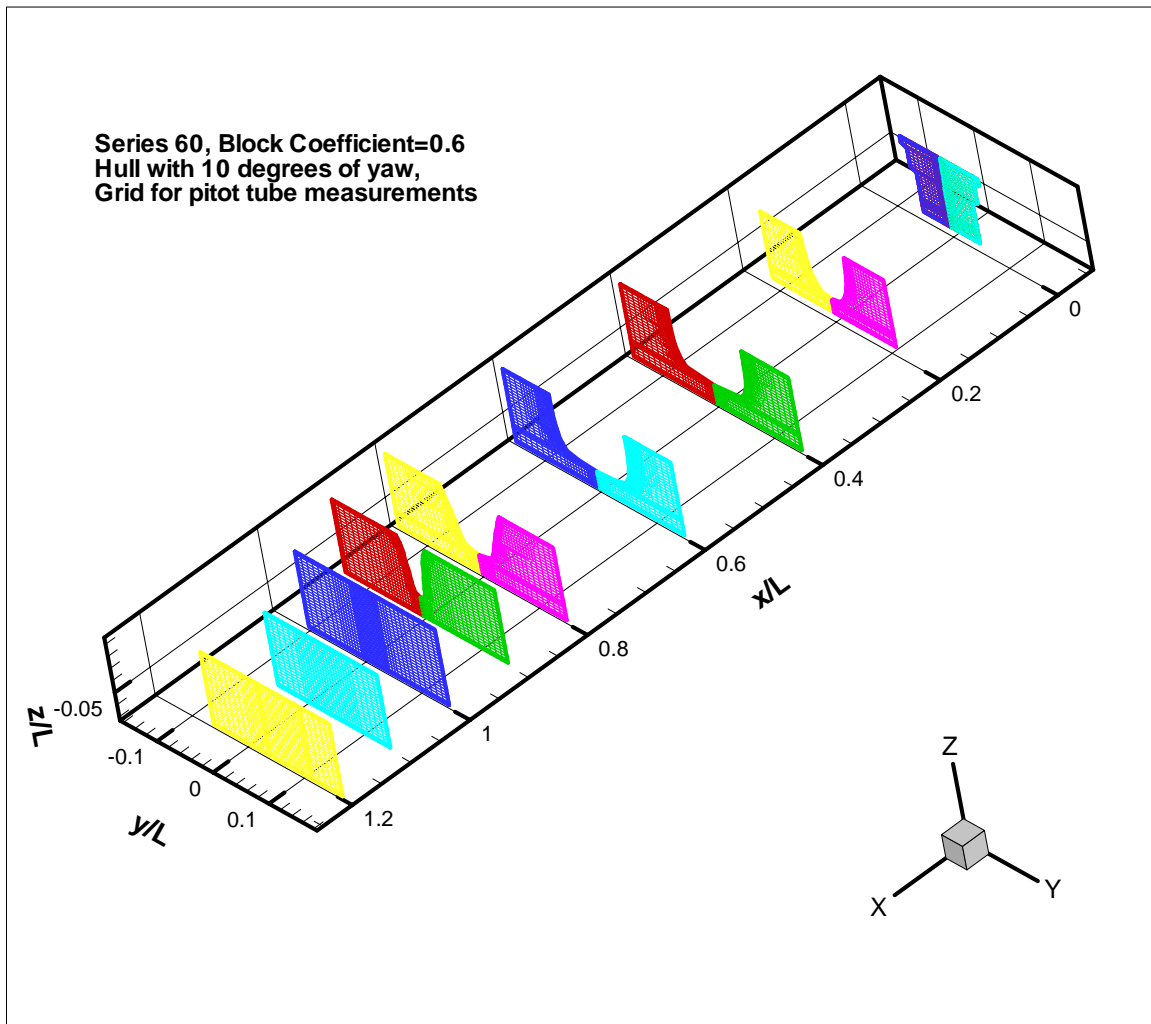
Figure 4, Measurement grid for Series 60, C_B=0.6 at 10 degrees yaw
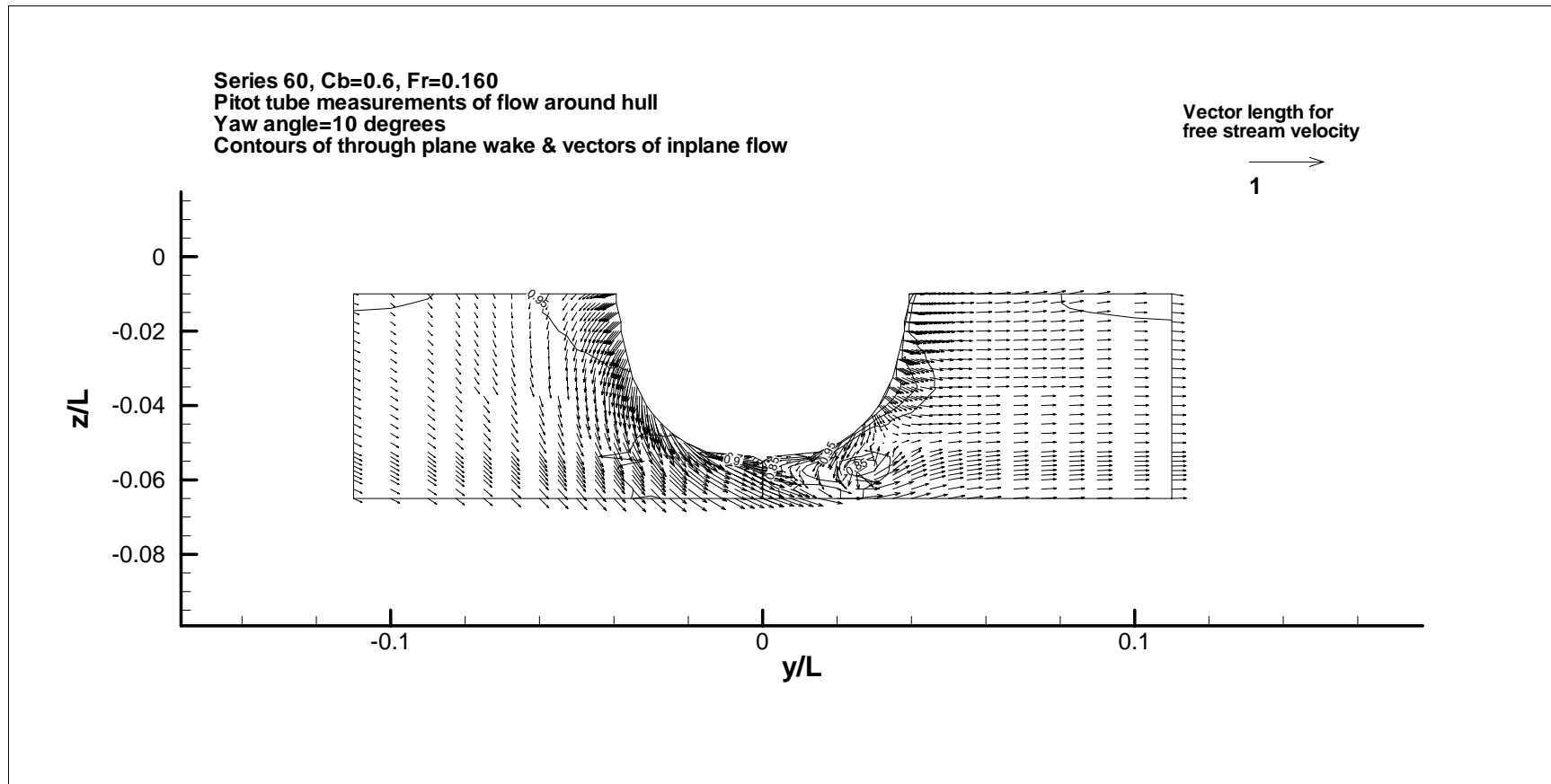
Figure 5, Results of pitot tube survey for flow around Series 60, C_B=0.6, section at 20%L
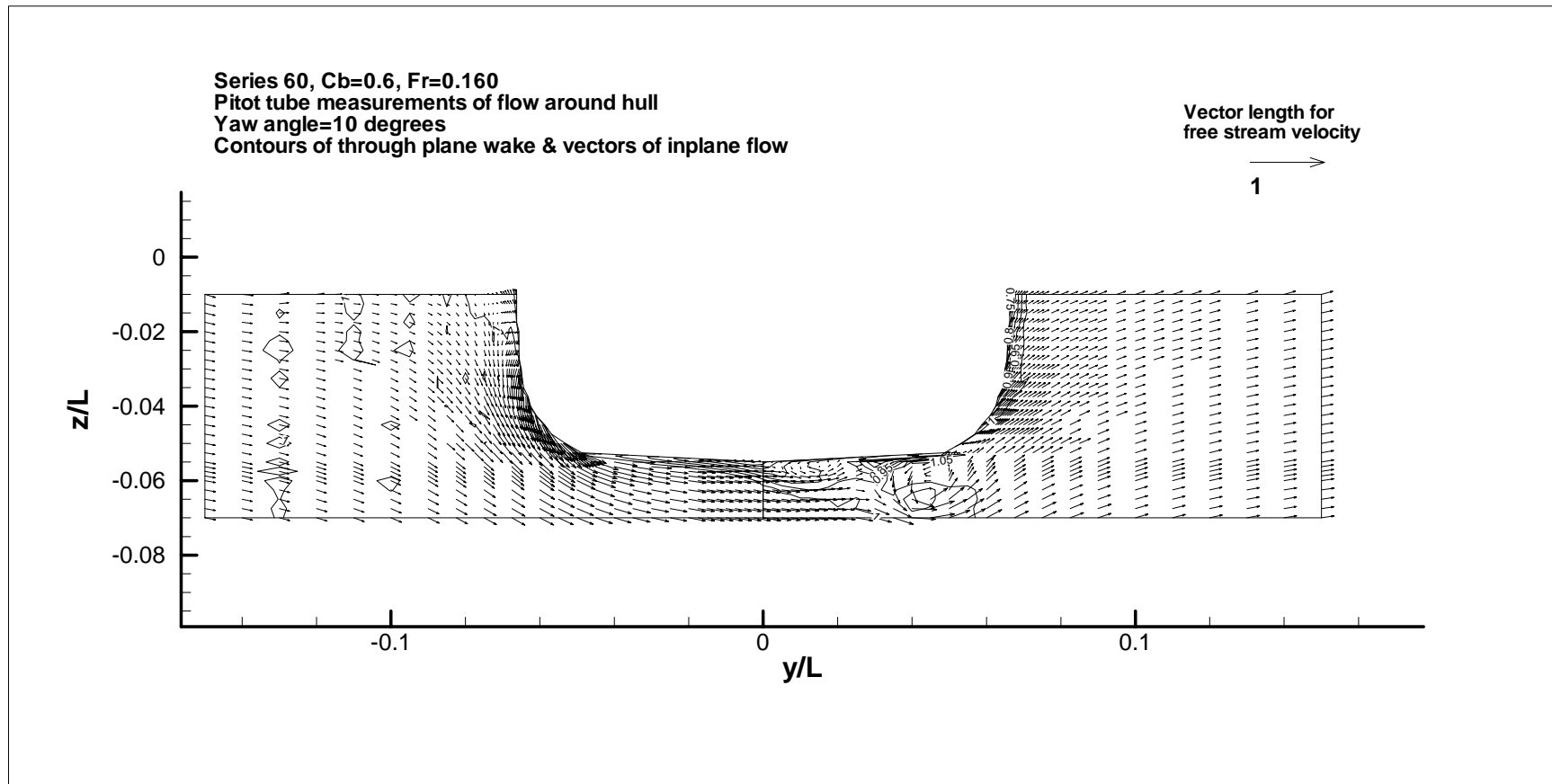
Figure 6, Results of pitot tube survey for flow around Series 60, C_B=0.6, section at 40%L

Series 60, Cb=0.6, Fr=0.160
Pitot tube measurements of flow around hull
Yaw angle=10 degrees
Contours of through plane wake & vectors of inplane flow

Vector length for
free stream velocity

1
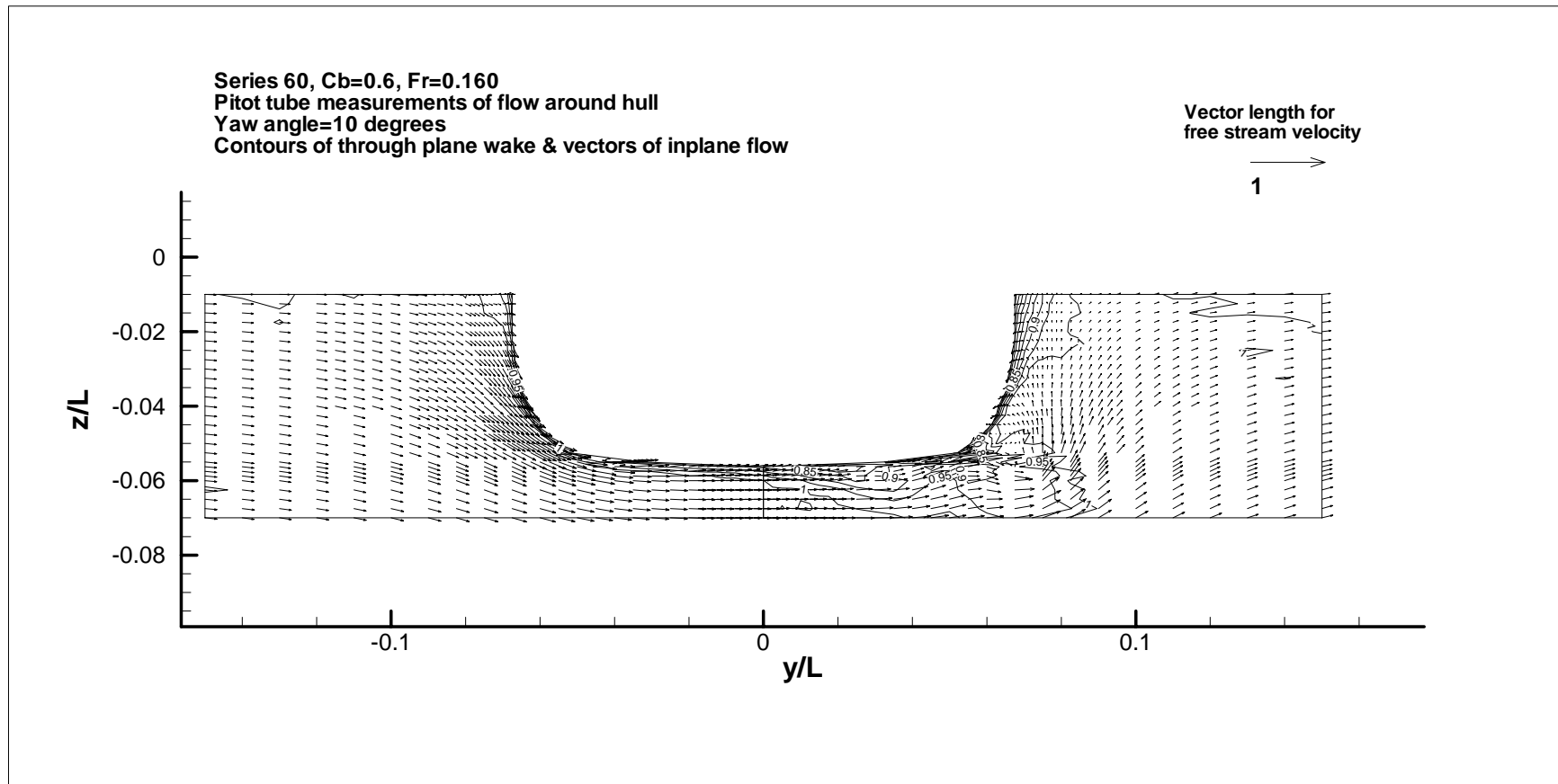
Figure 7, Results of pitot tube survey for flow around Series 60, C_B=0.6, section at 60%L

Series 60, Cb=0.6, Fr=0.160
Pitot tube measurements of flow around hull
Yaw angle=10 degrees
Contours of through plane wake & vectors of inplane flow

Vector length for
free stream velocity

1
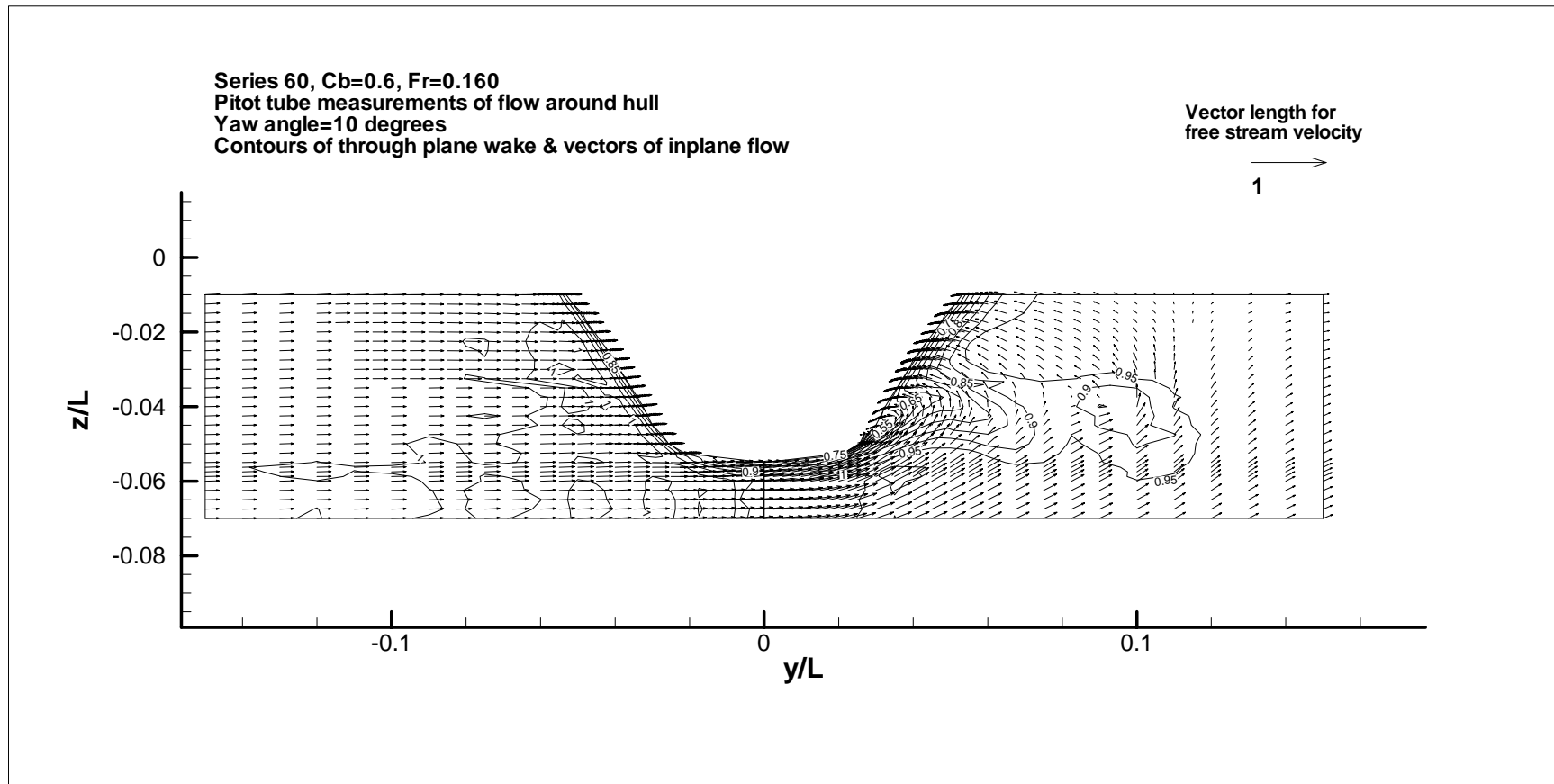
Figure 8, Results of pitot tube survey for flow around Series 60, C_B=0.6, section at 80%L

All these figures are for a Froude number of 0.16. The results for Froude number of 0.316 showed similar flow patterns. The Froude number of 0.16 was chosen because it was within the expected Froude number range for escort tugs, and was a close match to the speed used by Di Felice and Mauro (1999) for their experiments, which are discussed below.

LDV Data for Yaw Angle 35 Degrees

Di Felice & Mauro (1999) measured the flow around a double model of a Series 60 C_B=0.6 hull at a scale of 1:100 in a large cavitation tunnel using Laser Doppler Velocimetry (LDV). In this case, the model hull was symmetrical about the design waterline and the free surface effects were ignored. The yaw angle used was 35 degrees, which is within the expected range of operating yaw angles for an escort tug. The Froude number used for these experiments was 0.2, although the free surface was ignored. The flow speed for these experiments was 0.692 m/s.

The LDV used a two-component backscatter method, with estimated velocity resolutions within +/-1%. The flow was seeded with titanium dioxide particles, with a diameter of 1 μm. Measurements were made at two sections, 0.5L and 0.9L. The data density was 600 points for the first section and 800 points for the second. The measurements were made in the axis system of the tunnel, rather than normal to the centerline of the model. The resulting measurement planes were not at a constant location in ship axes, which was the convention used by Toda et al. (1992) and Longo and Stern (1996), but were normal to the direction of the undisturbed flow, rather than normal to the centreline of the ship. This was accepted in order to use the mechanized system for locating the measurement point within the flow, which was fixed in an axis system with the y and z-axes normal to the centerline of the cavitation tunnel. Also, the origin for the system was at the aft perpendicular for the model.

Measured flow vectors in the two planes are shown in Figure 9. Both planes are on the downstream side of the model. To be as consistent as possible with the presentation of results used by Longo and Stern (1996) geometric locations were non-dimensionalized by ship length, with the origin at the bow, and mean flow speeds were non-dimensionalized by the speed of the undisturbed flow. The resulting flow vectors for each plane are shown in Figures 9 and 10.

Series 60, Block coefficient=0.60
INSEAN data for flow at 35 degree yaw

Free stream
velocity, U

1
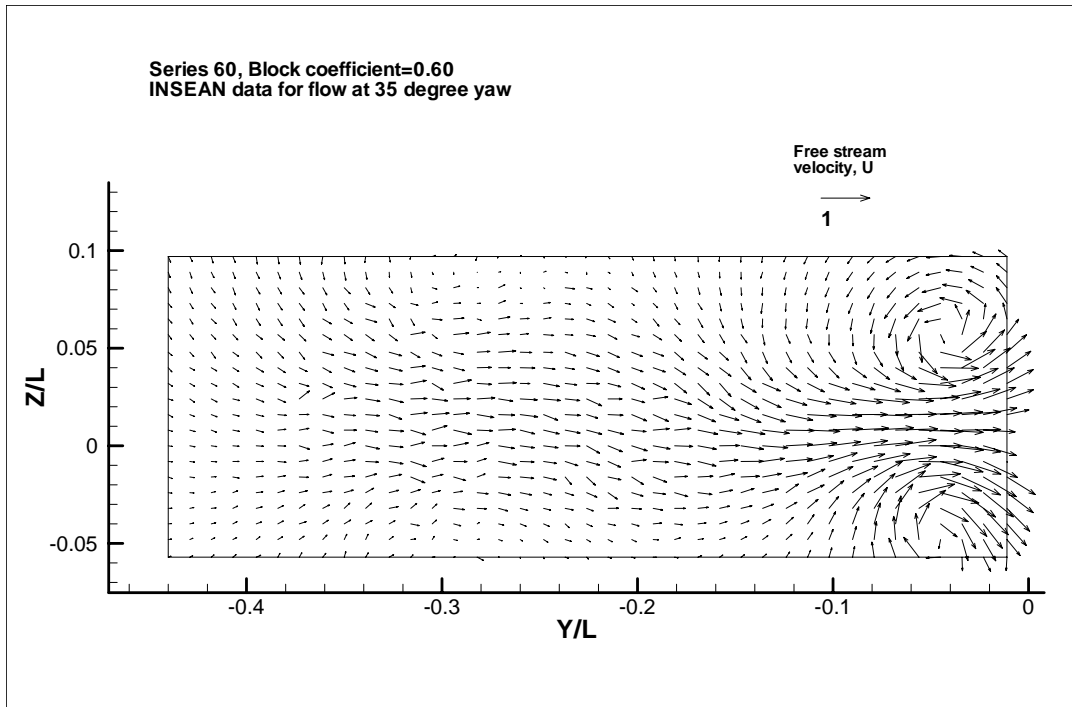
Figure 9, Flow vectors measured at 90%L, 35 degree yaw

Free stream velocity

1

Series 60, Cb=0.6,
INSEAN, 35 degree yaw
LDV data

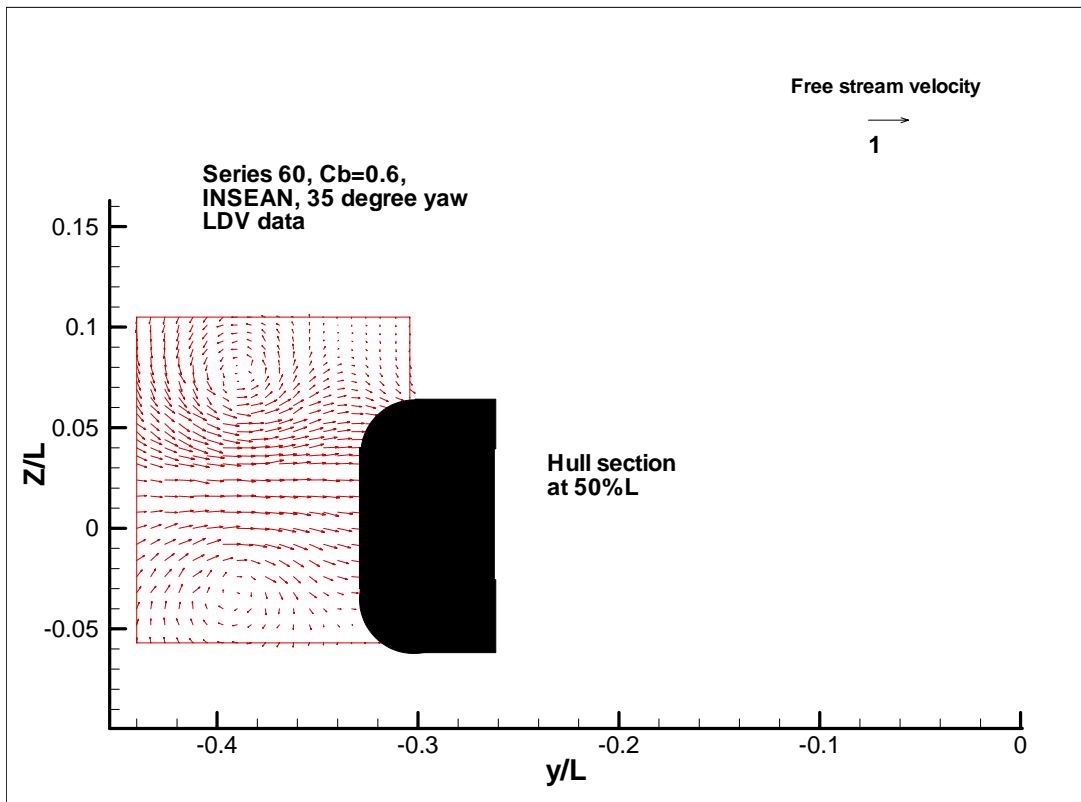**Hull section**
at 50%L

Figure 10, Flow vectors measured at 50%L, 35 degrees of yaw

Since the model was symmetrical about the waterline, the results given in Figures 9 and 10 should be symmetrical about the z/L value of zero, and this is the case, within an allowance for scatter in the results of the experiments (although it looks as though the model may have had a small pitch angle, since the two vortices in Figure 10 are not at the same z/L location).

Based on the geometry of the experiment, the maximum beam of the hull at 50%L was at a value of y/L approximately -0.34 and the maximum draft was at z/L of +/-0.059. Figure 10 shows the approximate locations of the maximum beam and maximum draft within the measurement coordinate system. Note that the origin used in these experiments was at the aft perpendicular and fixed in the axis of the cavitation tunnel, rather than the ship.

Results of the experiments were presented by Di Felice and Mauro (1999) as contours of cross flow velocities, vertical and transversal component standard deviation, Reynolds stresses, vorticity and vertical and transverse component skewness for the downstream side of the hull. The results showed distinct vortices at each plane. Di Felice and Mauro state that the advantage of the LDV method was the ability to measure quantities such as turbulence intensity and Reynolds stresses, as well as detailed measurements of the flow in the cross planes. All these results combined to give information on viscous and turbulent aspects of detached flow generated by the yawed hull.

CFD SIMULATIONS OF SERIES 60 CB=0.6 HULL WITH YAW ANGLE

Based on the results of the experiments some key features of flow patterns were around a Series 60 hull with a yaw angle were observed.

At 10 degrees:
- Closed contour of u velocity component that moves from centreline towards downstream side of the hull as flow moves further aft along hull
- Strong downward flow component on upstream side of hull, up to 60%L
- Strong upward flow component on downstream side of hull at 40%L and 60%L
- Strong circulating flow component on down stream side at 80%L

At 35 degrees:

- Strong circulating flow on downstream side of the hull at 50%L, which was not observed at 10 degrees
- Strong circulating flow on downstream side of hull at 90%L

Note that for the experiments at a yaw angle of 35 degrees, only in-plane velocity components were measured due to the nature of the instrumentation. Also, the change in the orientation of the measurement plane will affect the observed results. The flow patterns will look different, due to the different sections used, even if the flow is the same. This makes comparing the results slightly more complicated, but the actual measurement sections can be used in the CFD simulations.

It is important that CFD simulations capture the elements of the flow that were observed in the experiments. Different modelling strategies (number size and shape of mesh elements) were attempted until, accurate and numerically stable solutions were obtained.

Prismatic Model

For a ship with a large amount of parallel middle body, it is possible that the flow around the midsection can be modelled using a constant section prismatic approximation to the geometry. Reducing the hull model to a constant section can simplify the creation of the mesh, since only one face needs to have a detailed mesh, and the third dimension is created from uniform elements in the third dimension.

To model the case of a ship with yawed flow, the prismatic section was based on the midship section of the Series 60 C_B=0.6 hull. The angle between the incoming flow and the hull (yaw angle) was set by adjusting the boundary conditions, so that the velocity at the inlet planes had two components. The pressure outlet planes were set so that the backflow pressure was also in the same direction. The advantage of this approach was that one mesh could be used for all the yaw angles. Another simplification was to ignore the effect of the free surface. This was done to simplify the generation of the mesh and because the data from Di Felice and Mauro (1996) was for a double model, where the free surface was ignored.

This approach was useful in learning to use the meshing program (*GAMBIT*) and the CFD solver (*FLUENT*). Factors such as changing mesh size and shape were investigated and the results compared. Other factors that were investigated using the simple prismatic model were the number of elements along the circumference of the hull required to define realistic flow patterns. From this preliminary work, it was found that rectangular hexahedral mesh elements were the most promising approach. Thirty cells between the centreline and the waterline were found to give flow patterns that changed an acceptable amount with yaw angle, based on the results of the 3-dimensional model experiments. Tetrahedral elements were investigated with this simple geometry, but it was found that these introduced weak circulating flow on the downstream side of the hull at 10 degrees yaw angle, that was not observed in the three-dimensional model experiments. This may have been introduced due to error propagation caused by the non-orthogonal nature of the cells.

The factor that severely limited the application of this approach was that it is not possible to remove the effects caused by the flow entering the domain. Since the dominant flow direction was along the centreline of the model, even for yaw angles of 35 degrees, the flow was never actually steady along the length of the section. Lengthening the domain and increasing the yaw angle reduced the effect of the entrance somewhat, but never removed it.

Prismatic Model with Simple Bow

The next level of refinement was to include a simple bow on the prismatic section. This modification meant that uniform flow entered the computational domain and was not immediately influenced by the hull section. A bow that was simple to create using GAMBIT was a circular bow, based on revolving the constant section. It was thought that the simplified bow shape would not be as sensitive to yaw angle as a more conventional bow, since the flow would always separate.

The prismatic section used was based on the midship section of a 1:40 scale model of the Series 60. A summary of the mesh geometry and flow conditions is given in Table 3. The mesh is shown in Figure 11. The origin was at the bow, with flow components in the positve x and positive y directions. Again, the free surface was ignored, and so the mesh stopped at the nominal waterline for the hull.
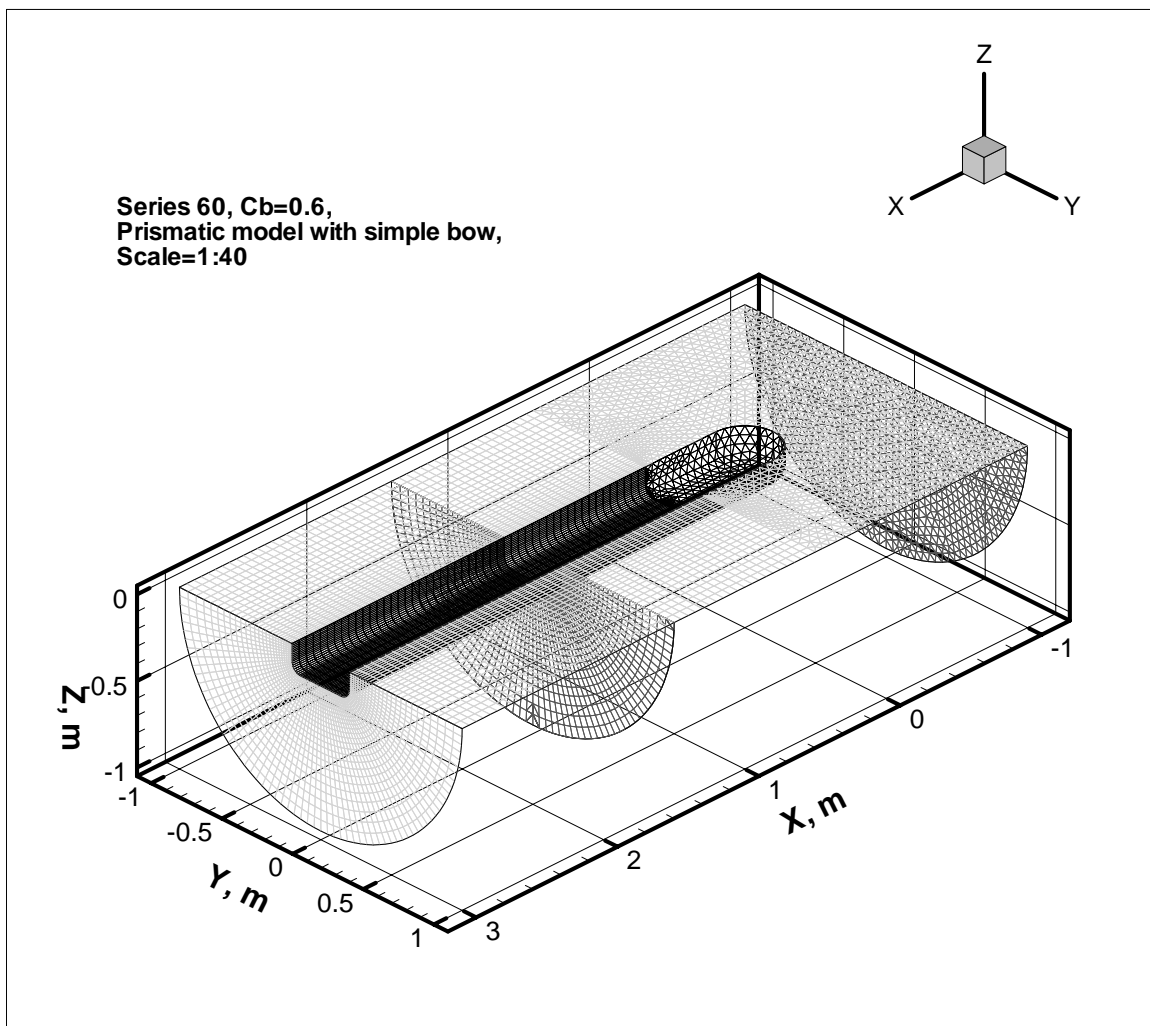

Figure 11, Mesh for prismatic hull with simple bow

| | Length, m | Beam, m | Draft, m | |
	X axis	Y axis	Z axis	Radius, m
Hull prism	3.000	0.406	-0.163	0.060
Bow	0.203	0.406	-0.163	0.060
Overall	3.203	0.406	-0.163	0.060
Boundary	4.000	+/- 1.000	-1.000	1.000

Section, m	Mesh at section	Mesh forward of this section
3	Quadrilateral	Hexahedral
0.5	Quadrilateral	Hex/Tet
0	Triangle	Tetrahedral
-1	Triangle	

Table 3, Summary of geometry and mesh for prismatic model with simple bow

The prismatic section of the hull had 33 uniformly spaced elements between the centreline and the waterline. The external boundary (which was a semi-circle) had the same number of elements. The radius was meshed with 25 elements, with an expansion ratio of 1.064 (so that the elements close to the hull were smaller than the elements at the boundary. The region from 0.5m to 3.0m was meshed with hexahedral elements. Between 0.5m and zero, the elements were changed to hybrid hexahedral and tetrahedral elements, and forward of the origin the region was meshed with tetrahedral elements. The total number of elements was approximately 195,000. The mesh was symmetrical about the centreline. No boundary layer cells were used.

Predictions of the flow were obtained using *FLUENT*. Uniform flow entered the domain through a velocity inlet on the upstream boundaries and exited through a pressure outlet on the downstream boundaries. The hull surface was defined as a no-slip wall and the waterline was defined as a slip wall. The flow speed was 0.875 m/s. Yaw angle was changed by varying the direction of the flow vector at the boundary using a cosine component for flow along the centreline and a sine component for flow normal to the centreline on the inlet out outlet. The turbulence model used was a $\kappa-\omega$ model with the default parameters. Turbulence intensity and turbulent viscosity ratios were set at 1% and 1 respectively. The flow was solved for the steady state case. Convergence limit was set to 10^{-3} (default values) for all parameters. All solutions converged within these limits.
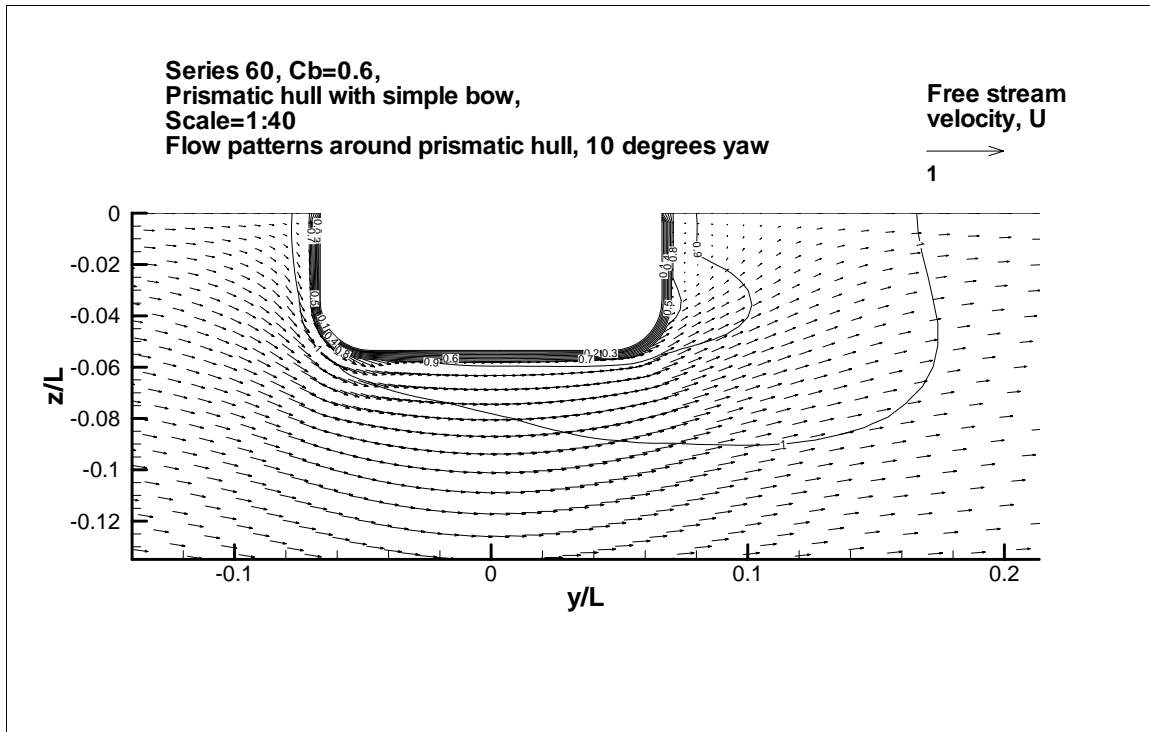
Figure 12, Flow around prismatic hull with simple bow, yaw angle 10 degrees (ship axis)
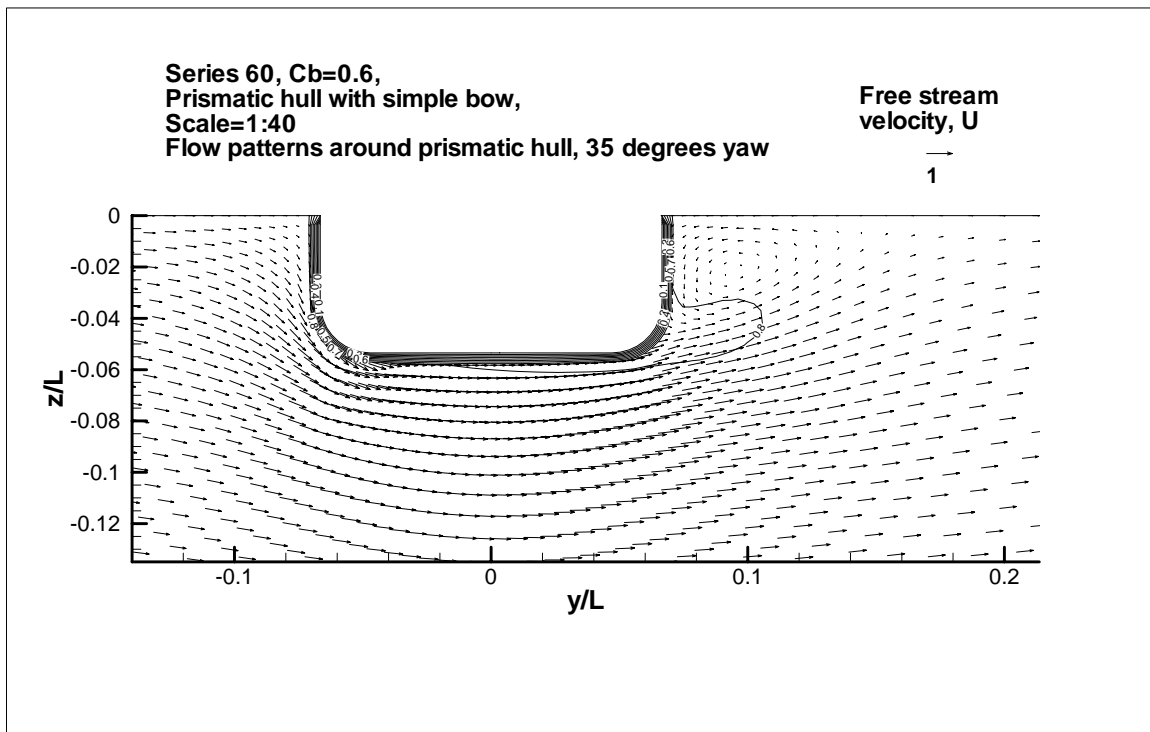

Figure 13, Flow around prismatic hull with simple bow, yaw angle 35 degrees (ship axis)

Flow components (countours of u/U and vectors based on flow components (v/U and w/U) for yaw angles of 10 degrees and 35 degrees in the ship based coordinate system (used by Longo and Stern, 1996) are shown in Figures 12 and 13 respectively at a section 1.703m aft of the forward section of the hull (x/L=0.56) in the ship-based axis system. This location was chosen since the flow downstream of this point changed very little for both yaw angles, and it was approximately half the length of the actual model down stream from the end of the waterline.

The flow measurements made by Di Felice and Mauro (1996) at 35 degrees of yaw were obtained in a flow based axis system with the origin at the stern (and x positve towards the bow), rather than a ship based axis system with the origin at the bow (and x positive towards the stern). A comparison of the measurement planes in the two systems for the prismatic model with a simple bow is shown in Figure 14. The ship-based grid in the ship-based plane is shown in red and the grid in the flow-based plane is shown in grey.
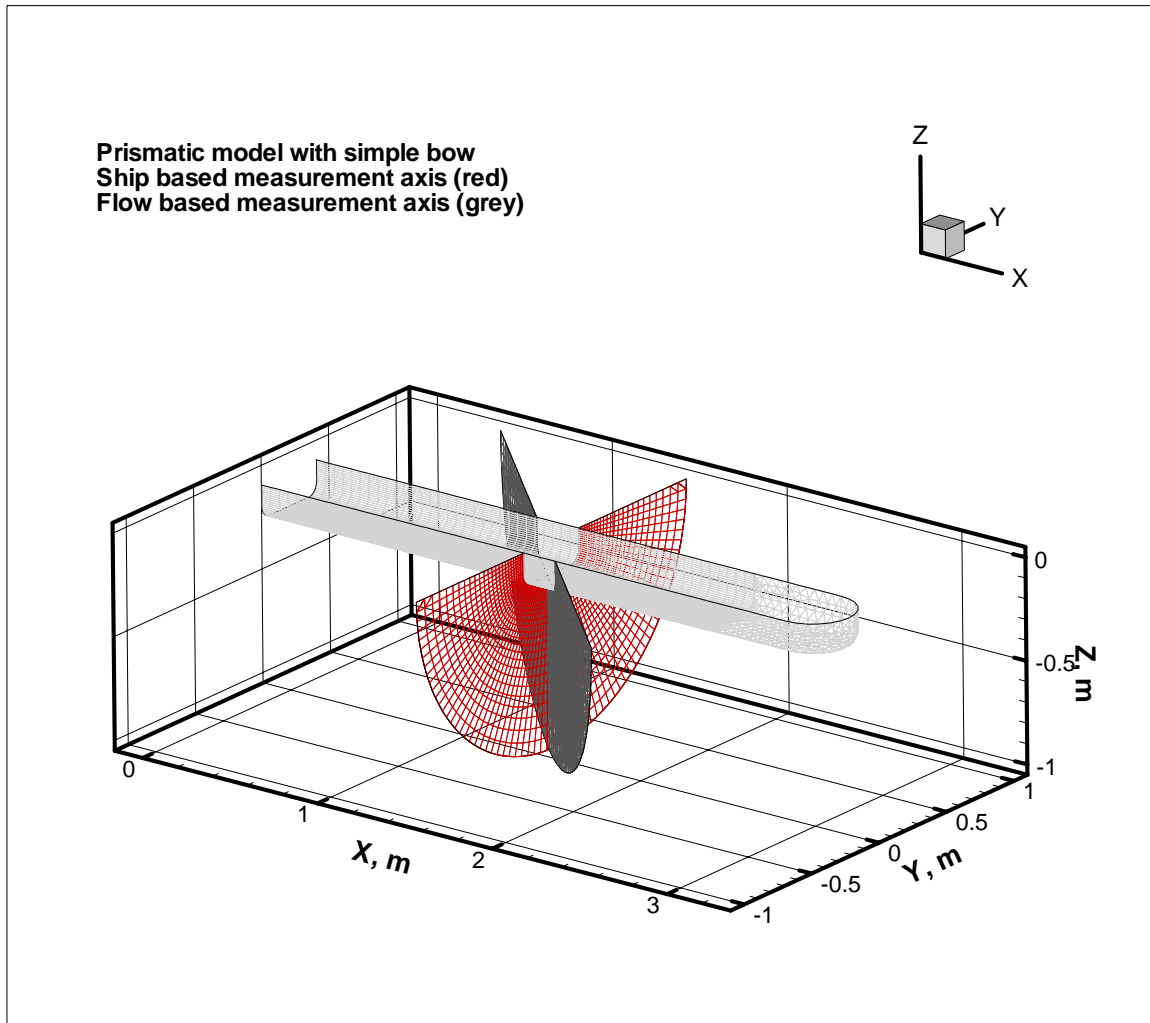

Figure 14, Ship based axis system (red) and flow based axis system (grey)

The velocity components obtained in flow axis plane were given by *FLUENT* in the original (ship-based) grid axis system. The results at 35 degrees of yaw required some manipulation before they were comparable with the experiments. The origin was moved so that it corresponded to a point 3.048m aft of the forward edge of the bow (the aft perpendicular for the model, with x direction positive towards the bow) and the flow components were reflected to match the orientation used in the experiments (negative flow components in x and y directions). Once the origin had been moved and the flow directions changed, the resulting flow vectors and associated grid points within the measurement plane were transformed into the in-plane and through-plane velocity components using the following unit vector transformations;

$$\vec{i} = Cos\theta.\vec{i}\,' - Sin\theta.\vec{j}\,'$$
$$\vec{j} = Sin\theta.\vec{i}\,' + Cos\theta.\vec{j}\,'$$

where;
i and j are unit vectors in the grid based coordinates and
i' and j' are unit vectors in the flow based coordinates and
θ is the angle between the flow direction and the grid based coordinates.

Since the transformation about the vertical axis was rotation, the third axis (z in the experiment notation) was unchanged.

The predicted flow patterns in the flow based axis system are shown in Figure 15. In this case the contours are in the direction of the free-stream flow and vectors give the predicted in-plane velocity components for a plane through the hull normal to the direction of the flow. The free stream velocity of 0.875 m/s was used to non-dimensionalize all of the flow velocity components. The region shown was picked to overlap with the results of the experiments given in Figure 10.
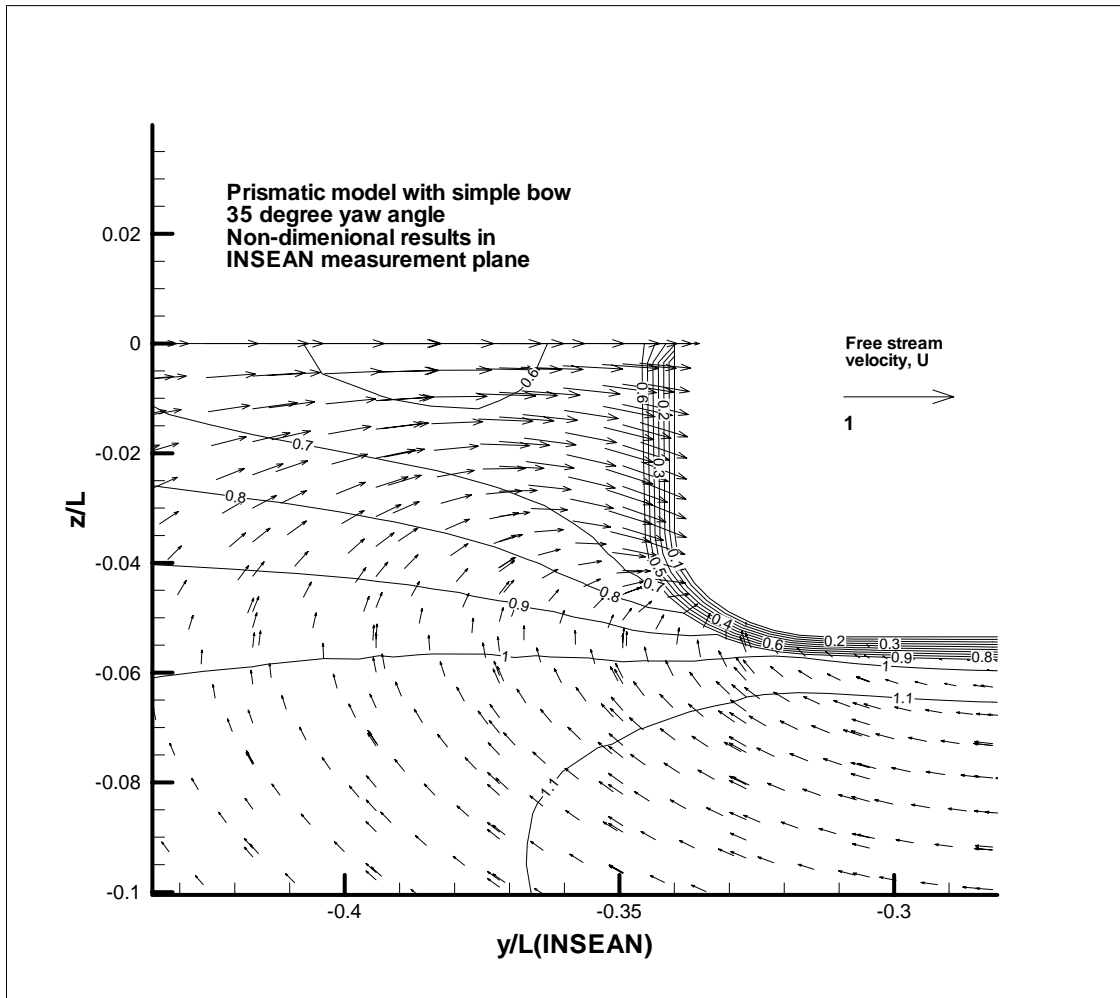
Figure 15, Flow around prismatic hull with simple bow, yaw angle 35 degrees (flow axis)

The flow around the simple model at 10 degrees of yaw, shown in Figure 12, can be compared to the flow around the three-dimensional model shown in Figures 6 and 7. Note that no measurements were made at 50%L in the experiments and the Series 60 hull does not actually have any parallel middle body, and so the comparison is a little subjective.

The CFD predictions capture many of the important flow features of the in-plane velocity components. Figure 12 shows an area of weak flow on the downstream side of the hull, with almost no circulation. The flow patterns around the up-stream and downstream bilge are also well predicted.

The velocity component through the plane (u/U) shown in Figure 12 does not show the same characteristics as the model experiments. The flow contours at 10 degrees of yaw do not show the well-developed flow pattern close to the downstream bilge radius, which was observed in the model experiments. The simulations do predict the development of

some asymmetry in the flow contours on the downstream side, but the predicted flow has a more uniform distribution that that observed in the model experiments. This feature may be a result of the bow shape, and the finer bow of the actual Series 60 model is probably having an effect on the longitudinal flow component.

The predictions for 35 degrees of yaw for the simplified model, given in Figure 15 can be compared with the experiment results in Figure 10. No through plane velocities were measured in the experiments, so the comparison is limited to the in-plane velocities. Here the comparison is not as good. Although the flow patterns close to the waterline are reasonably well predicted, the CFD prediction does not show the formation of the closed vortex off the downstream bilge. It is not clear if this is due to an inadequate grid, or the simplification of the hull form.

Figures 12 and 13 show CFD predictions for yaw angles of 10 degrees yaw and 35 degrees, based on the same (ship based) axis system. These figures show the development of the circulating flow on the downstream side of the hull. At 10 degrees of yaw, the circulating flow is very weak and close to the hull surface. As the yaw angle was increased, the speed of the flow components increased, and the centre of the vortex moved away from the hull.

The model using simplified geometry appears to predict many important features of the flow quite well, when compared in a subjective way to the results of the three dimensional experiments. These simulations were useful in establishing the validity of the meshing strategy and gaining experience with the meshing software and CFD solver.

Series 60 Hull

The final step was to consider a full three-dimensional model of the Series 60 $C_B=0.6$ hull. Given that one data set did not have a free surface, and the second data set was available for a relatively low Froude number (0.16) it was not necessary to model the free surface. As a result the mesh for the fluid could have a fixed boundary at the static waterline for the hull.

A surface file for the Series 60 $C_B=0.6$ had been previously used at IOT for construction of a 1:20 scale model. This file was used as the starting point for generating the mesh within *GAMBIT*. The hull was trimmed to the static waterline prior to meshing. The surfaces were imported into *GAMBIT* as virtual surfaces. Small edges were removed and any edges of surfaces that did not match were connected. Also some surfaces defined in the original geometry were merged to make the meshing easier. The next step was to add the boundary conditions. Different approaches were tried, including rectangular and semi-cylindrical boundary conditions. The overall volume was constructed from sub-volumes in order to complete the meshing.

Both tetrahedral and hexahedral mesh elements were tried for cell shapes within the mesh. Meshing the hull with hexahedral elements over most of the ship was relatively straight forward, especially with the semi-cylindrical boundary condition. However, joining the hexahedral mesh to the tetrahedral mesh proved to be more challenging, and determining a suitable face size for the interface was largely a matter of trial and error.

The final result given here was for the hull up to the waterline in a tank with semi-cylindrical boundary conditions. The mesh used was made up of hexahedral elements over most of the length of the hull and tetrahedral elements at the bow and stern. The origin for the hull surface was located where the aft perpendicular for the ship intersected the keel and the centreline, with x positive towards the bow, y positive to starboard and z positive upwards. This coordinate system was retained as the origin for the mesh. The mesh was created in *GAMBIT* with dimensions in metres for the full size ship, and scaled to 1:40 using the scaling functions in *FLUENT*.

The mesh consisted of 14 sub-volumes symmetrical about the centreline and an additional volume at the bow, for a total of 15. The basic hexahedral mesh consisted of 12 elements equally spaced between the centreline and the waterline along the outer radius of the cylinder. The same number of equally spaced elements was created at the hull. The radius was divided into 15 elements. The spacing of these elements varied with the longitudinal position along the hull. Over most of the hull (the four sub-volumes at the aft end of the hull) the expansion ratio was 1.064. This ratio was reduced for the last two volumes, since this was found to give larger element on the faces where the hexahedral mesh joined the tetrahedral mesh. The end volumes were meshed with tetrahedral/hybrid elements. At the stern, there were two volumes, symmetrical about the centreline, but at the bow, it was a single volume. The hexahedral mesh extended from 10%L to 98.7%L forward of the aft perpendicular, for a total percentage of 88.7%L

meshed with hexahedral elements. A summary of overall ship and mesh geometry is given in Table 4.

The number of elements in the mesh was 17,280 hexahedral elements and approximately 680,000 tetrahedral and hybrid elements.

Ship	
Length BP, m	121.92
Length, WL, m	123.93
Beam, m	16.256
Draft, m	6.502

Basic Mesh Boundary	x m	y min m	y max m	z min m	z max m
Inlet	200	-80	80	-73.498	6.502
Hex mesh	120.275	-80	80	-73.498	6.502
Hex mesh	12.192	-80	80	-73.498	6.502
Outlet	-50	-80	80	-73.498	6.502

Table 4, Summary of mesh geometry, Series 60, C_B=0.6

This basic hexahedral mesh was too coarse to predict the flow accurately. Before solving for the flow patterns, the mesh was refined within *FLUENT*. The regions that were refined are given in Table 5. The final refined mesh had 48 elements at the hull surface. The final mesh is illustrated in Figures 16 and 17.

Refined mesh Region	x min m	x max m	y min m	y max m	z min m	z max m
One level	20	110	-28	28	-18	6.502
Two level	20	110	-20	14	-12	6.502

Table 5, Summary of refined mesh

Series 60, Cb=0.6, Fr=0.160,
CFD simulations for flow around hull,
Yaw angle=10 degrees
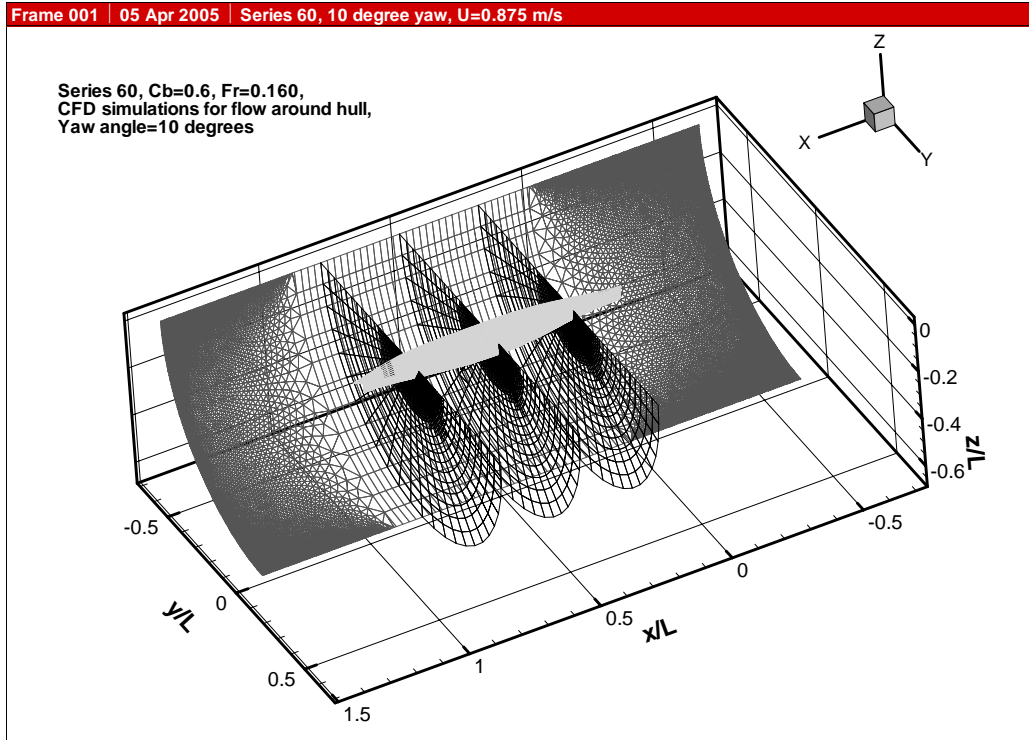
Figure 16, Overall mesh geometry for Series 60, C_B=0.6

Series 60, Cb=0.6, Fr=0.160,
CFD simulations for flow around hull,
Yaw angle=10 degrees
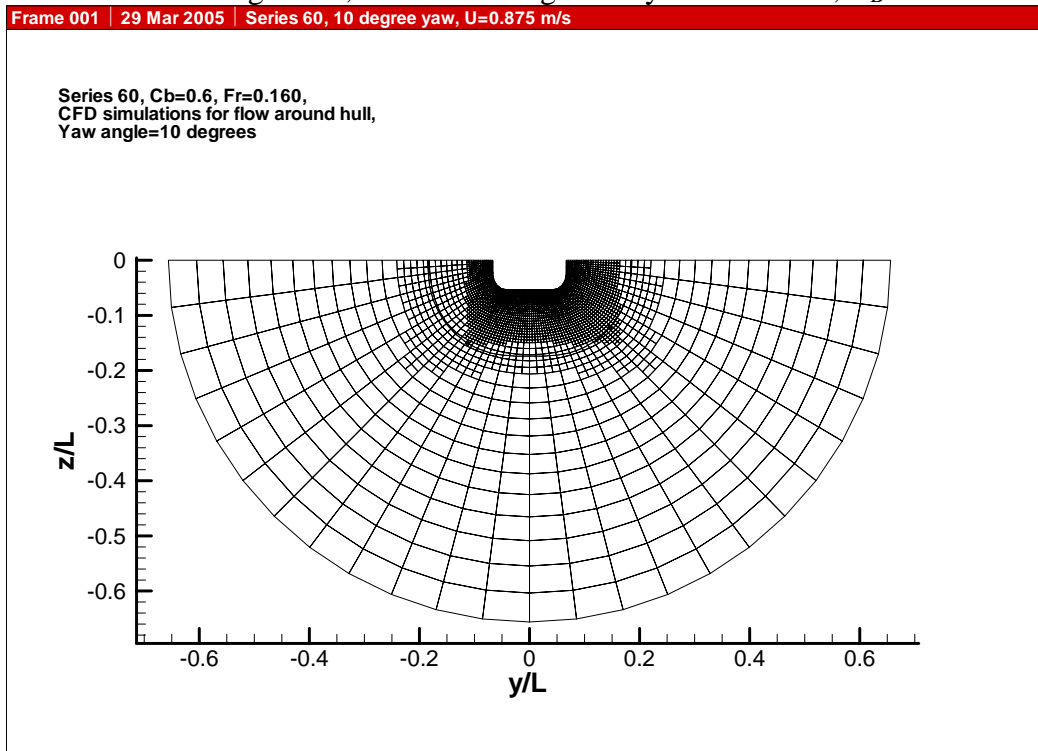
Figure 17, Section through mesh for Series 60, C_B=0.6

The upstream end and upstream side were defined as velocity inlets and the downstream end and downstream side were defined as pressure outlets. The hull and the free surface were defined as walls.

Predictions of the flow were obtained using *FLUENT*. Uniform flow entered the domain through a velocity inlet on the upstream boundaries and exited through a pressure outlet on the downstream boundaries. The hull surface was defined as a no-slip wall and the waterline was defined as a slip wall. The flow speed was 0.875 m/s. Yaw angle was changed by varying the direction of the flow vector at the boundary using a cosine component for flow along the centreline and a sine component for flow normal to the centreline on the inlet out outlet. The turbulence model used was a $\kappa-\omega$ model with the default parameters. Turbulence intensity and turbulent viscosity ratios were set at 1% and 1 respectively. The flow was solved for the steady state case. Convergence limit was set to 10^{-3} (default values) for all parameters. All solutions converged within these limits *(not true yet...)*.

For 10 degrees of yaw, the results of the CFD simulations were converted to the coordinate system used during the experiments (Longo & Stern 1996), which required the origin to be moved to the forward perpendicular of the ship at the waterline, and the x and y axes to be reflected. Flow speeds were non-dimensionalized using the free stream flow speed, and presented as contours of longitudinal flow velocity and vectors of in plane flow velocity. Predicted flow patterns for sections at 20%L, 40%L, 60%L and 80%L are given in Figures 18 to 21. These predictions are comparable to the results of the model experiments (Longo and Stern, 1996) shown in Figures 5 to 8.

Figure 18, CFD predictions of flow around Series 60, C_B=0.6, 10 degree yaw, section at 20%L (ship axis)
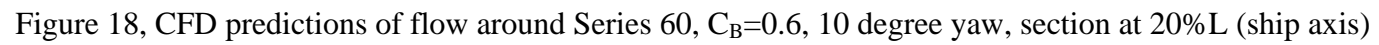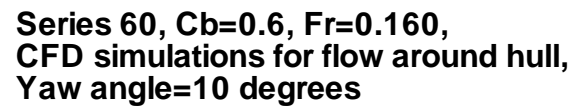
Figure 19, CFD predictions of flow around Series 60, C_B=0.6, 10 degree yaw, section at 40%L (ship axis)

Figure 20, CFD predictions of flow around Series 60, C_B=0.6, 10 degree yaw, section at 60%L (ship axis)
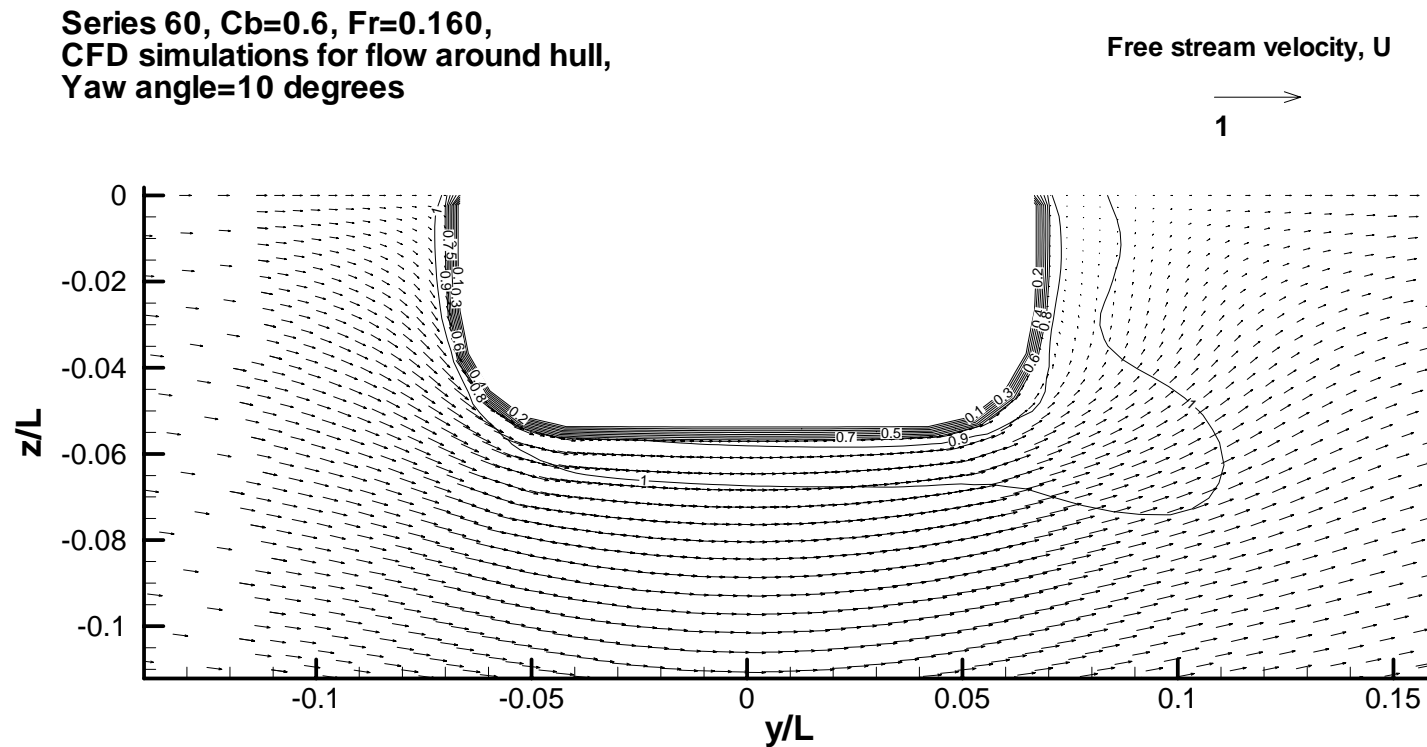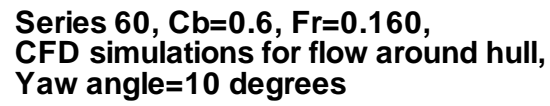
Figure 21, CFD predictions of flow around Series 60, C_B=0.6, 10 degree yaw, section at 80%L (ship axis)

The coordinate system used by Di Felice and Mauro (1999) was closer to the system used in the definition of the mesh. The only change required was to move the origin in the z direction, from the keel to the waterline. The predicted velocity components were non-dimensionalized by the free stream velocity, and geometry was non-dimensionalized by ship length. A plane was created within the solution to match the plane used in the model experiments at 35 degree yaw (Di Felice and Mauro, 1999), and the results were transformed from the ship based axis system to the flow based axis system, using the same transformations discussed above. The CFD predictions at the 50%L section are shown in Figure 22. The equivalent results in the ship based axis system are shown in Figure 23. This figure illustrates the differences in the observed flow patterns caused by the change in measurement plane.
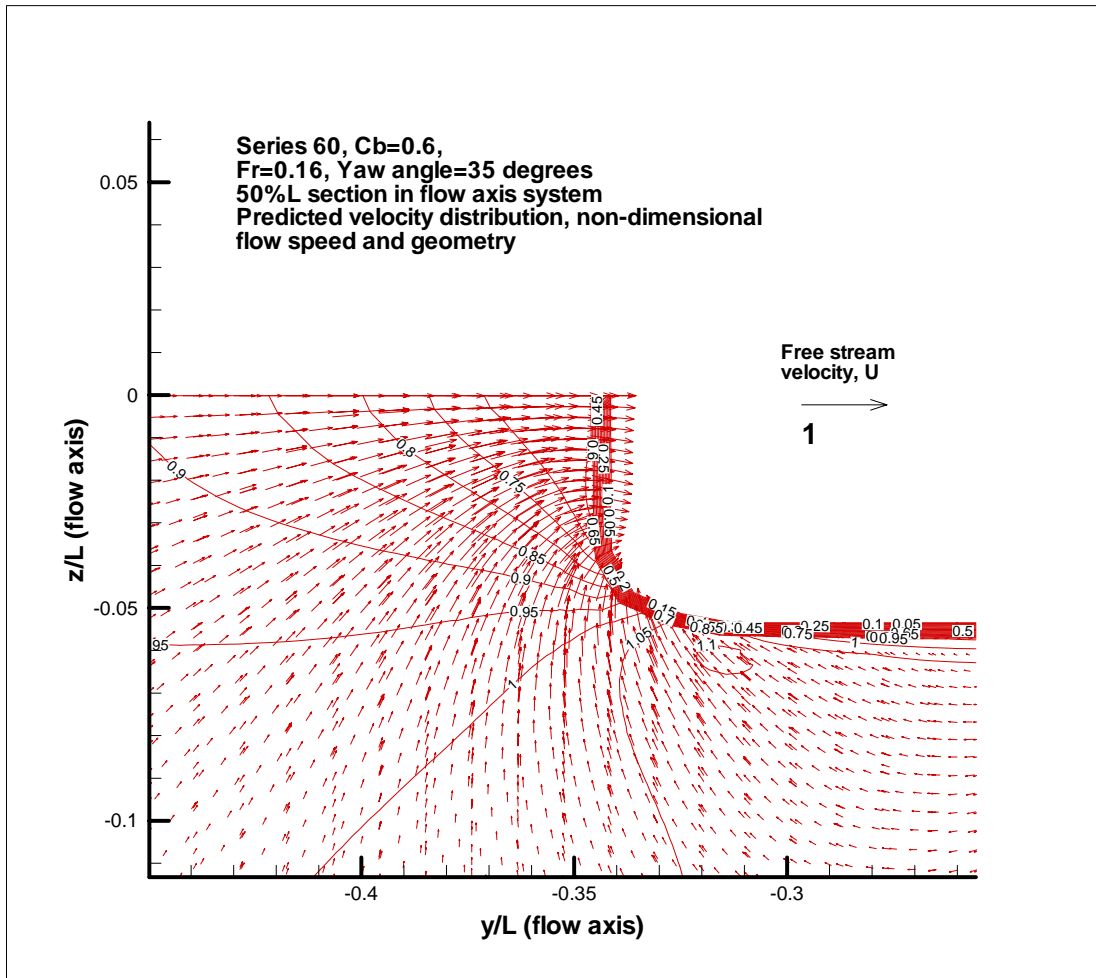

Figure 22, CFD predictions of flow around Series 60, C_B=0.6, 35 degree yaw, section at 50%L (flow axis)
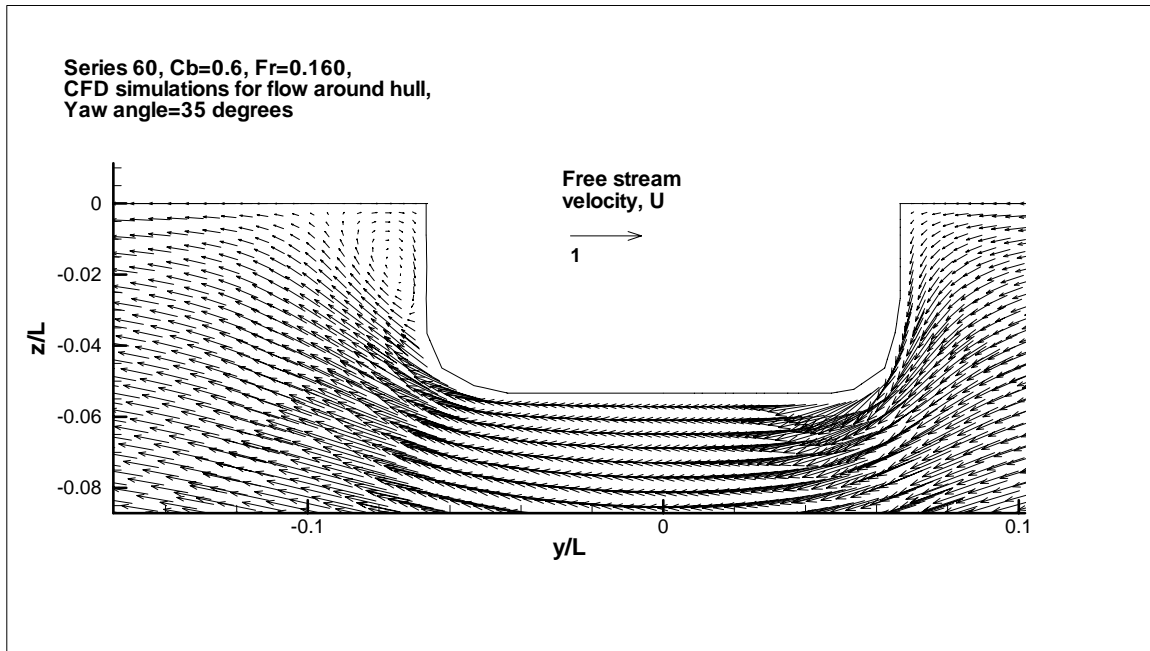
**Series 60, Cb=0.6, Fr=0.160,
CFD simulations for flow around hull,
Yaw angle=35 degrees**

**Free stream
velocity, U**

1

z/L

0

-0.02

-0.04

-0.06

-0.08

-0.1

0

0.1

y/L

Figure 23, CFD predictions of flow around Series 60, C_B=0.6, 35 degree yaw, section at 50%L (ship axis)

DISCUSSION OF RESULTS

The CFD simulations present in this report were the author's first attempt to obtain realistic flow predictions for a 3-dimensional hull using a commercial CFD code. Much of the meshing for the hull was the result of trial and error, and several unsuccessful attempts to mesh the hull were made prior to obtaining the values given in this report.

In many ways, the predictions of the flow patterns are good. The best predictions are for the in-plane flow velocities at 10 degrees of yaw. At all sections where experiment results are presented, the predicted flow vectors show similar patterns to the experiments for large areas of the results. The flow patterns are well predicted on the upstream side of the hull, and on the downstream side of the hull from the waterline down to the mid depth point.

There are some areas where the flow predictions are not good. In no case does the CFD mesh used predict the formation of the vortices on the underside of the keel clearly seen in the results of the experiments at 20%L, 40%L and 60%L. At 80%L the CFD results shows good agreement with the experiments for the flow patterns close to the downstream side of the hull, but does not predict the formation of the separated vortex centred at approximately y/L of 0.09 and z/L of –0.045. At all sections the boundary layer is under predicted by the CFD mesh.

For 35 degrees of yaw, the CFD predictions were not as good. The data set is smaller, but at 50%L, there is a very strong vortex seen on the downstream side of the hull. The CFD predictions show that this flow pattern was starting to form, but the predicted flow does

not form a closed loop, that was seen in the model experiments. Based on the presentation of the results in the ship-based axis system, it appears that the CFD mesh is under predicting the size of the vortex on the downstream side of the hull.

It is quite likely that the mesh used in this report can be refined further to improve the quality of the results. The hull surfaces imported were very small, and the complete surface was made up of many very small surfaces. When imported surfaces were merged, the original vertices remained, which constrained the meshing process. Also, it is likely that the final mesh is still too coarse.

The comparisons discussed in this report are subjective. For a more rigorous comparison it will be necessary to develop a numerical procedure for comparing experiment data with CFD predictions, and between CFD predictions where mesh sizes or other numerical parameters are changed. Some preliminary work suggests that an analysis procedure will have to be written. The likely form for this will be to import both sets of data, interpolate them both on a common grid and compare numerical values over the complete grid. It will then be possible to develop error maps where the magnitude of the difference between the two sets of results is mapped

A preliminary concept of this approach is shown in Figure 24, which shows the difference between the experiment values at 60%L and the CFD predictions, in terms of the magnitude and direction of the through plane velocity components, non-dimensionalized by the free stream speed.
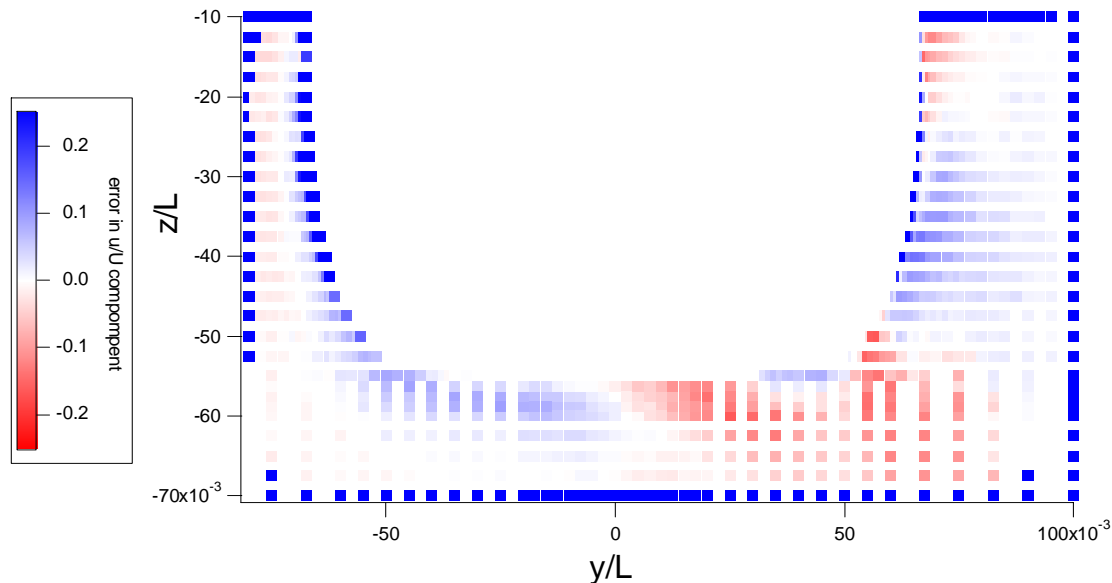

Figure 24, Preliminary error map for through-plane velocity component
(grid based on experiment measurement points)

ACKNOWLEDGEMENTS

REFERENCES

Allan, R. and Molyneux, D. 'Escort Tug Design Alternatives and a Review of Their Hydrodynamic Performance', World Maritime Technology Conference, Society of Naval Architects and Marine Engineers, Paper A11, September 2004.

Di Felice, F. and Mauro, S., 'LDV Cross-Flow Survey on a Series 60 Double model at Incidence', Proceedings of 9th International Offshore and Polar Engineering Conference, Brest France, May 30-June 4, 1999, pp. 536-543.

ITTC, 'Report of the Resistance and Flow Committee', 18th International Towing Tank Conference, Kobe, Japan, pp 47-92.

Tahara, Y., Longo, J. & Stern, F., 'Comparison of CFD and EFD for the Series 60 C_B=0.6 in Steady Drift Motion', *Journal of Marine Science and Technology*, Vol. 7, 2002 pp. 17-30.

Toda, Y., Stern, F. & Longo, J., 'Mean-Flow Measurements in the Boundary Layer and Wake and Wave Field of a Series 60 C_B=0.6 Ship Model-Part 1: Froude Numbers 0.16 and 0.316', Journal of Ship Research, Vol. 36, No. 4. Dec. 1992, pp. 360-377.

Longo, J. Stern, F. & Toda, Y., 'Mean-Flow Measurements in the Boundary Layer and Wake and Wave Field of a Series 60 C_B=0.6 Ship Model-Part 2: Scale Effects on Near-Field Wave Patterns and Comparisons with Inviscid Theory', *Journal of Ship Research*, Vol. 37, No. 1. Jan. 1993, pp. 16-24.

Longo, J. & Stern, F., 'Yaw Effects on Model-Scale Ship Flows', Proceedings, 21st Symposium on Naval Hydrodynamics, June 24-28, Trondheim, Norway, 1996, pp. 312-327